

Cite this: *Chem. Sci.*, 2025, **16**, 14242

All publication charges for this article have been paid for by the Royal Society of Chemistry

Received 21st May 2025  
Accepted 28th June 2025DOI: 10.1039/d5sc03694a  
rsc.li/chemical-science

## Introduction

The recent discoveries of molecular compounds of uranium in the +2 oxidation state<sup>1–11</sup> have opened a route to explore new reactivity in uranium chemistry. Notably, it has resulted in a few unambiguous examples of single-metal oxidative addition examples involving both two and four electron transfer to N=N (e.g. in azobenzene, Fig. 1a and b) and C=C (e.g. in phenyl-acetylene)  $\pi$ -bonds.<sup>8,12</sup> Examples of both intramolecular<sup>13–16</sup> C–H activation and intermolecular<sup>17</sup> C–H oxidative addition (Fig. 1c) by putative U(II) intermediates have also been reported. More recently examples of two-electron oxidative atom and group transfer reactions at a well-defined uranium(II) centre have also been reported.<sup>9,18</sup> These examples suggest that

<sup>a</sup> Institut des Sciences et Ingénierie Chimiques, Ecole Polytechnique Fédérale de Lausanne (EPFL), 1015 Lausanne, Switzerland. E-mail: marinella.mazzanti@epfl.ch

<sup>b</sup> Centro de Química Estrutural, Institute of Molecular Sciences, Instituto Superior Técnico, Universidade de Lisboa, 2695-066 Bobadela, Portugal

<sup>c</sup> Laboratoire de Physique et Chimie des Nano-objets, Institut National des Sciences Appliquées, 31077 Toulouse, Cedex 4, France

<sup>d</sup> X-Ray Diffraction and Surface Analytics Platform, Institute of Chemical Sciences and Engineering (ISIC), École Polytechnique Fédérale de Lausanne (EPFL), 1015 Lausanne, Switzerland

<sup>e</sup> Laboratory for Quantum Magnetism, Institute of Physics, Ecole Polytechnique Fédérale de Lausanne (EPFL), 1015 Lausanne, Switzerland

<sup>f</sup> ADSResonances Sàrl, 1920 Martigny, Switzerland

† Electronic supplementary information (ESI) available: For detailed syntheses, spectroscopic, magnetic and crystallographic data. CCDC 2411215, 2411216, 2411217. For ESI and crystallographic data in CIF or other electronic format see DOI: <https://doi.org/10.1039/d5sc03694a>

## Facile N–C bond cleavage and arene reduction by a transient uranium(II) complex†

R. A. Keerthi Shivarao, <sup>a</sup> Leonor Maria, <sup>b</sup> Thayalan Rajeshkumar, <sup>c</sup> Rosario Scopelliti, <sup>d</sup> Ivica Živković, <sup>e</sup> Andrzej Sienkiewicz, <sup>ef</sup> Laurent Maron <sup>c</sup> and Marinella Mazzanti <sup>\*a</sup>

Complexes of uranium(II) remain extremely rare and their reactivity is practically unexplored. Here we report that the reduction of the heteroleptic bis-aryloxide U(III) complex  $[\text{U}(\kappa^6-({}^t\text{Bu}_2\text{ArO})_2\text{Me}_2\text{-cyclam})]\text{I}$ , A, yields a rare and highly reactive U(II) intermediate that enables a rare example of intramolecular uranium mediated N–C cleavage and effects arene reduction resulting in the isolation of the U(IV) complex  $[\text{U}(\kappa^5-({}^t\text{Bu}_2\text{ArO})\text{Me}_2\text{-cyclam})\{\kappa^2-({}^t\text{Bu}_2\text{ArOCH}_2)\}]\text{ (2)}$  and of the inverse–sandwich complex  $[\{\text{U}(\kappa^5-({}^t\text{Bu}_2\text{ArO})_2\text{Me}_2\text{-cyclam})\}_2(\mu-\eta^6\cdot\eta^6\text{-benzene})]\text{ (3)}$  respectively. Moreover, the U(II) solvent-dependent reactivity results in the formation of a putative U–N<sub>2</sub> complex in diethyl ether. Computational, EPR and magnetic studies indicate the electronic structure of **3** to be an equilibrium between two possible electronic structures very close in energy: (U(IV)–arene<sup>4–</sup>–U(IV) and U(III)–arene<sup>2–</sup>–U(III)). These results indicate that polydentate amine-phenolate ligands can be used to access highly reactive U(II) intermediates and that provides evidence that U(II) species are involved in the formation of inverse sandwich complexes.

oxidative addition reactivity may be easily accessible for uranium compounds in the +2 oxidation state, but the study of these complexes is limited by their scarce number and their high reactivity.

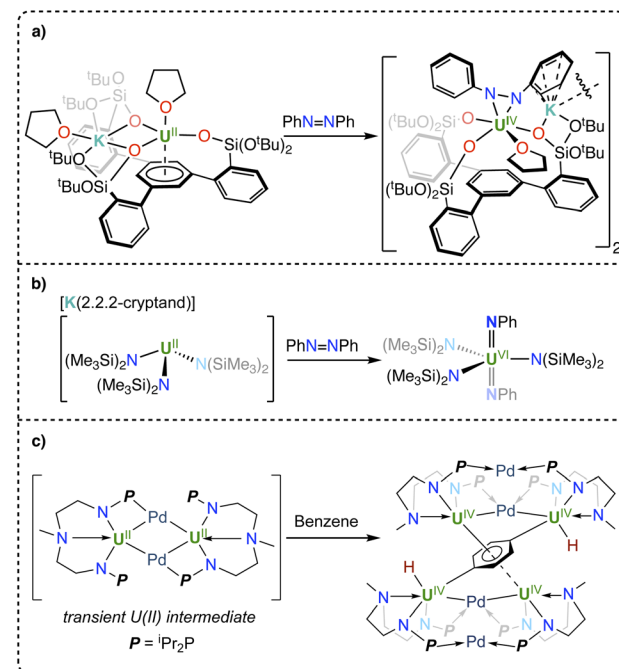


Fig. 1 Previously reported oxidative addition reactions featuring U(II) complexes.



Single-metal oxidative-additions reactions play a key role in d-block metal chemistry and in transition metal mediated catalysis.<sup>19</sup> In contrast, these reactions are hard to reach in f element chemistry because of their limited access to two electron redox couples and multielectron transfer.<sup>20,21</sup> Notably, uranium mediated oxidative addition reactions have been for a long time limited to single electron transfer. Fewer cases of N≡N, N=N and N-N oxidative additions involving multiple electron transfer are also known, although the reaction intermediates remain in many case unidentified.<sup>22–27</sup> Redox active ligands<sup>8,9,28–31</sup> and sterically induced reductions (SIR)<sup>32,33</sup> have provided a successful alternative metal-ligand cooperative approach to implement oxidative addition at a single metal centre.

In contrast, examples of metal-based oxidative addition reactions at a single uranium centre, not involving oxidative atom or group transfer, remain scarce<sup>12,20,21</sup> but recent reports<sup>8,12,17</sup> indicate that U(II) compounds are well poised to develop this chemistry.

Moreover, U(II) species are also likely intermediates in the formation of uranium inverse sandwich complexes,<sup>34–36</sup> however evidence of their involvement is still lacking due to the high reactivity of putative intermediate species. Notably, prior to the isolation of the first example of a U(II) complex by Evans in 2013,<sup>2</sup> attempts to isolate molecular complexes of uranium in the +2 oxidation state by reduction of the U(III) analogues in aromatic solvents had resulted in the isolation of inverse sandwich complexes with uranium in a formal +2 oxidation state. However, further spectroscopic and computational studies indicated that the electronic structure of these complexes is better described as U(III)-arene<sup>2–</sup>–U(III) or U(IV)-arene<sup>4–</sup>–U(IV).<sup>36,37</sup> The possible involvement of intermediate "U(II)" species in the formation of inverse sandwich complexes still remains to be proven.

So far, stabilisation of U(II) species has been attained with bulky cyclopentadienyl derivatives preventing access to the metal centre<sup>2–5,14,15,38</sup> or with arene anchored polydentate ligands that can establish strong delta bonding interactions with the uranium centre.<sup>1–10</sup> The only example of a U(II) complex with a strong N-donor ligand set  $-\text{N}(\text{SiMe}_3)_2$  that did not present high steric crowding<sup>4</sup> was isolated at low temperature and was found to be extremely reactive towards C–H activation of the  $-\text{N}(\text{SiMe}_3)_2$  ligand resulting in the cyclometalated U(III) complex  $[\text{U}\{\text{N}(\text{SiMe}_3)_2\}_2(\kappa_2\text{-C,N-CH}_2\text{SiMe}_2\text{NSiMe}_3)]$ .<sup>39</sup> Amine-phenolate ligands of different charge, bulk and denticity were shown to be well suited for isolating well defined and highly reactive U(III) complexes<sup>40,41</sup> but have so far failed to produce complexes of uranium in lower oxidation state. We became interested in investigating U(III) to U(II) reduction using the polydentate aminophenolate ligand  $(^t\text{Bu}^2\text{ArO})_2\text{Me}_2\text{-cyclam}$ . This was prompted by the reported ability of the heteroleptic bis-aryloxide U(III) precursor  $[\text{U}(\kappa^6\{(^t\text{Bu}^2\text{ArO})_2\text{Me}_2\text{-cyclam}\})\text{I}]$ , A<sup>41</sup> to cleave azobenzene yielding the U(VI) bis-imido complex  $[\text{U}\{(^t\text{Bu}^2\text{OAr})_2\text{Me}_2\text{-cyclam}\}\{\text{NPh}\}_2]$  and the U(IV) byproduct  $[\text{U}\{(^t\text{Bu}^2\text{OAr})_2\text{Me}_2\text{-cyclam}\}\text{I}]$ . While a different mechanism was proposed based on the seminal work of Burns,<sup>26</sup> the possibility of a U(II) intermediate in this reaction cannot be ruled out. Here

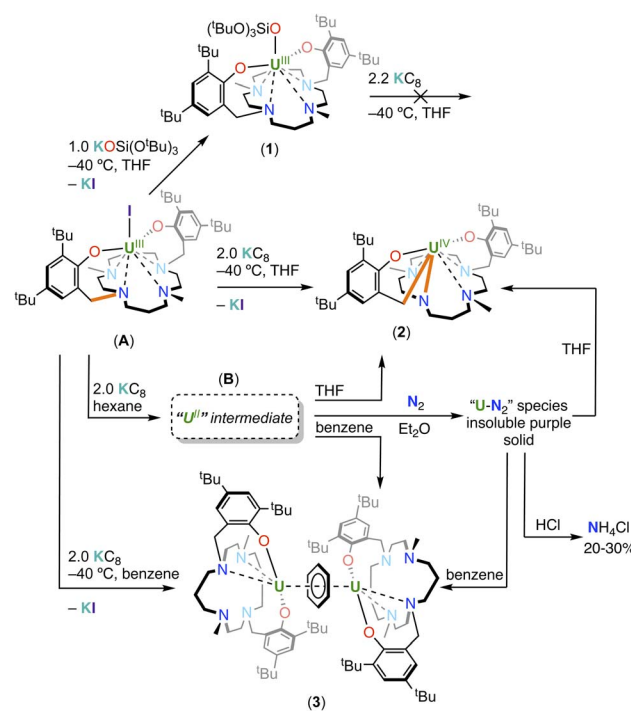
we provide evidence that reduction of the complex A produces a highly reactive U(II) intermediate enabling arene reduction and the first example of uranium(II) mediated N–C cleavage. We also report the synthesis and reduction of the analogous complex  $[\text{U}(\kappa^6\{(^t\text{Bu}^2\text{ArO})_2\text{Me}_2\text{-cyclam}\})(\text{OSi}(\text{O}'\text{Bu})_3)]$  (1) to elucidate the importance of the presence of a reactive halide position for generating neutral U(II) species supported by non-carbon based ligands. It should be noted that, to date, most reported U(II) complexes are "ate" complexes probably due to the rarity of stable heteroleptic U(III) precursors.<sup>3,7</sup>

## Results and discussion

### Synthesis of a heteroleptic U(III) complex

With the bis-aryloxide U(III) precursor  $[\text{U}(\kappa^6\{(^t\text{Bu}^2\text{ArO})_2\text{Me}_2\text{-cyclam}\})\text{I}]$  (A) in hand, we first prepared the heteroleptic dark red brown U(III) complex  $[\text{U}(\kappa^6\{(^t\text{Bu}^2\text{ArO})_2\text{Me}_2\text{-cyclam}\})(\text{OSi}(\text{O}'\text{Bu})_3)]$  (1) in 56% yield from the salt metathesis reaction between A and  $\text{KOSi}(\text{O}'\text{Bu})_3$  (see Scheme 1 below).

Single crystals suitable for X-ray diffraction (Fig. 2) were grown from slow evaporation of a solution of 1 in pentane at  $-40\text{ }^\circ\text{C}$ , while bulk isolation was performed from a concentrated reaction mixture in hexane at  $-40\text{ }^\circ\text{C}$ . The  $^1\text{H}$  NMR spectrum of 1 in  $d_8\text{-THF}$  at  $-40\text{ }^\circ\text{C}$  (Fig. S4†) displays 35 peaks between 43 ppm and  $-50\text{ ppm}$ , which corresponds well with the  $^1\text{H}$  NMR spectrum of the crude reaction mixture (Fig. S3†) in  $d_8\text{-THF}$  at  $-40\text{ }^\circ\text{C}$ , indicating a straightforward ligand displacement reaction. The solid-state molecular structure of 1 (Fig. 2) features a seven-coordinate U(III) ion bound by two oxygens from the two aryloxide arms, four nitrogen atoms of the cyclam



Scheme 1 Synthesis of complexes 1, 2 and 3 (bonds involved in oxidative addition are drawn in orange).

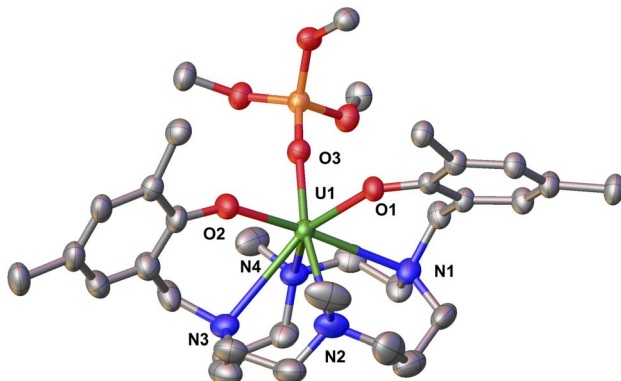


Fig. 2 Molecular structure of complex **1** with thermal ellipsoids drawn at the 50% probability level. Methyl groups of *t*Bu group and hydrogen atoms have been omitted for clarity.

ring and a tris(*tert*-butoxy)siloxide ligand in a distorted pentagonal bipyramidal geometry. The U–O<sub>aryloxide</sub> bond distances in **1** (2.251(4) Å and 2.309(4) Å), although slightly longer presumably to the presence of the siloxide ligand, are still comparable to the U(*III*) precursor **A**<sup>41</sup> (2.223(4) Å and 2.263(3) Å). The U–N<sub>cyclam</sub> bond distances in **1** (2.797(6) Å, 2.824(5) Å, 2.909 (6) Å, 2.953(6) Å; average U–N<sub>cyclam</sub> = 2.87(6) Å) are slightly longer than those in **A** (2.721(5) Å – 2.809(5) Å; average U–N<sub>cyclam</sub> = 2.76(5) Å).

### Reduction of U(*III*) complexes

The reduction of the U(*III*) complexes **A**<sup>41</sup> and **1** was pursued in order to explore the possibility of accessing a uranium(*II*) complex. The <sup>1</sup>H NMR spectrum in *d*<sub>8</sub>-THF of the reaction mixture obtained after reacting **1** with 1–2.2 KC<sub>8</sub> at –40 °C (Fig. S7a and S8b†) after 14 hours showed the presence of the resonances of **1** and of minor decomposition products suggesting that its reduction was not possible in the investigated conditions.

In contrast, the reaction of a violet solution of complex **A** with excess KC<sub>8</sub> (2.2 equiv.) in *d*<sub>8</sub>-THF at –40 °C led to the complete disappearance of the signals assigned to **A** in the <sup>1</sup>H NMR spectrum (Fig. S12†) and the appearance of a new set of resonances. Single crystals of the U(*IV*) complex [U{ $\kappa^5$ -[*t*Bu<sub>2</sub>ArO]Me<sub>2</sub>-cyclam}]{ $\kappa_2$ -[*t*Bu<sub>2</sub>ArOCH<sub>2</sub>]} (**2**) suitable for X-ray diffraction were isolated from a concentrated reaction mixture in THF at –40 °C (Fig. 3). The easier reduction of **A** compared to **1** is most likely due to the presence of the reactive iodide ligand that is easily eliminated upon reduction with KC<sub>8</sub>. In contrast, reduction of the complex **1** would require the formation of an “ate” complex which is not accessible in the reducing conditions used.

Analytically pure complex **2** was isolated in 45% yield from a concentrated hexane solution of the reaction mixture. The <sup>1</sup>H NMR spectrum of **2** in *d*<sub>8</sub>-THF at –40 °C features 39 peaks from 230 ppm to –273 ppm (Fig. S13†). Complex **2** was observed as the major species formed even when the reaction was conducted in the presence of one equiv. of 2,2,2-cryptand. The solid-state structure of **2** shows that the reduction of **A** with KC<sub>8</sub>

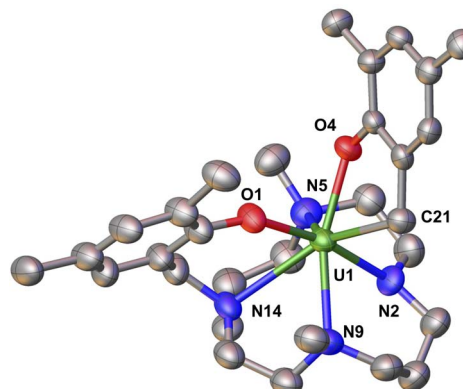


Fig. 3 Molecular structure of complex **2** with thermal ellipsoids drawn at the 50% probability level. Methyl groups of *t*Bu group and hydrogen atoms have been omitted for clarity.

did not lead the formation of a stable divalent uranium species as anticipated, but resulted in a U(*IV*) complex derived from the reductive C–N cleavage of one ligand arm.

Notably, the benzylic C–N bond connecting the cyclam ring to the aryloxide arm is cleaved forming a new C–U bond. The formation of complex **2** is likely to involve a highly reactive putative U(*II*) species that undergoes intramolecular oxidative addition of the C–N bond to yield the respective U(*IV*) complex. The removal of the bound iodide in **A** as KI upon reduction opens a coordination site at the uranium centre that likely facilitates the intramolecular oxidative addition reaction, resulting in the seven-coordinate complex in **2**. Monitoring the reduction of K<sub>2</sub>(*t*Bu<sub>2</sub>ArO)<sub>2</sub>Me<sub>2</sub>-cyclam with 2.2 equiv. KC<sub>8</sub> by <sup>1</sup>H NMR spectroscopy (see ESI and Fig. S29†) did not show any evolution, and only unreacted starting material was observed; thereby ruling out the possibility of a ligand reduction occurring without metal assistance. The proposed oxidative addition mechanism invoking a putative U(*II*) species is further corroborated by the stability of the U(*III*) complex **1** under similar reducing conditions as those used for the formation of **2**.

Stoichiometric oxidative addition of the C–N bond to transition metals is well established and has been used to develop catalytic methodologies that have emerged recently as a powerful strategy for the preparation or utilization of nitrogen-containing compounds.<sup>42–47</sup> However, complex **2** represents only the second example of an oxidative addition of a C–N bond mediated by a uranium complex<sup>48</sup> and the first promoted by a monometallic putative uranium(*II*) species. In the only reported example of oxidative C–N addition to an f-element, Liddle and coworkers showed that the reduction of the mononuclear U(*IV*) complex [U(TsXy)(Cl)(THF)] [TsXy = HC-(SiMe<sub>2</sub>-NAr)<sub>3</sub>; Ar = 3,5-Me<sub>2</sub>C<sub>6</sub>H<sub>3</sub>] in hexane yielded the bimetallic U(*IV*)/U(*IV*) [U{HC(SiMe<sub>2</sub>Ar)<sub>2</sub>(SiMe<sub>2</sub>- $\mu$ -N)}( $\mu$ - $\eta^1$ - $\eta^1$ -Ar)U-(TsXy)] as a result of a bimolecular reductive C–N bond cleavage by a putative U(*III*) intermediate.<sup>48</sup> In the latter example only a one-electron transfer from each metal is involved resulting in an overall unchanged oxidation state. In contrast, the formation of **2** requires a two-electron transfer process at a single metal centre, a putative U(*II*), which results in the overall oxidation



state of the metal increases by +1 on going from U(III) to U(IV) reminiscent of transition metal promoted C–N oxidative addition.

The solid-state molecular structure of **2** (Fig. 3) reveals a uranium ion in the +4 oxidation state with an overall coordination number of seven, wherein the metal center is bound by three neutral amino nitrogen atoms from the cyclam ring, two anionic oxygens from the aryloxide arms, one anionic amido nitrogen and one monoanionic carbon atom resulting from the benzylic C–N bond cleavage. The U–O<sub>aryloxide</sub> bond distances in **2** ( $\text{U–O}_{\text{aryloxide}} = 2.177(6)$ ,  $2.219(6)$  Å) are shorter than those in **A** ( $2.223(4)$  and  $2.263(3)$  Å) in agreement with the ionic radii contraction expected for a U(IV) ion. The U–N<sub>cyclam-amine</sub> bond distances in **2** ( $2.599(9) – 2.779(9)$  Å; av.  $\text{U–N}_{\text{cyclam-amine}} = 2.68(2)$  Å) are also shorter than those in **A** ( $2.721(5)$  Å –  $2.809(5)$  Å; av.  $\text{U–N}_{\text{cyclam}} = 2.76(5)$  Å), but considerably longer than the U–N<sub>cyclam-amido</sub> bond distance ( $2.265(6)$  Å) in **2**.<sup>41</sup> The U–N<sub>cyclam-amido</sub> bond distance ( $2.265(6)$  Å) in **2** compares well with previously reported U(IV) amido bond distances.<sup>49–51</sup> The newly formed U(IV)–C<sub>cyclam</sub> bond distance ( $2.505(11)$  Å) is in the range of previously reported U(IV)-alkyl bond distances ( $2.4$ – $2.5$  Å)<sup>52–57</sup> and is similar to that found in a eight coordinate U-alkyl compound ( $2.5134(7)$  Å).<sup>58</sup>

Given the highly reactive nature of the putative U(II) species generated upon reduction we sought to investigate if dinitrogen reduction reactivity could compete with N–C cleavage by conducting the reduction of **A** with  $\text{KC}_8$  (2.2 equiv.) in a less coordinating solvent (diethyl ether) under  $\text{N}_2$ . The reaction was carried out at  $-40$  °C for 3 days and resulted in the formation of an insoluble purple species containing  $\text{N}_2$ -bound uranium species that was stable under vacuum. Dissolution of the purple species in THF or in benzene resulted in  $\text{N}_2$  release and formation of complex **2** (see ESI, Fig. S27†) and the inverse sandwich complex  $[\{\text{U}(\kappa^5\text{–}\{({}^t\text{Bu}_2\text{ArO})_2\text{Me}_2\text{-cyclam}\})\}_2(\mu\text{-}\eta^6\text{:}\eta^6\text{-benzene})]$ , **3** respectively (see *infra* and ESI, Fig. S26†).

We were not able to isolate any  $\text{N}_2$ -bound uranium complex, but we found that quenching the reaction mixture, resulting from the reduction reaction of **A** with 2.2 equiv. of  $\text{KC}_8$  in diethyl ether  $-40$  °C under  $\text{N}_2$ , with a strong acid (HCl in diethyl ether) revealed (upon quantitative integration performed with dimethyl sulfone as the internal standard) the formation of ammonium chloride in 20% yield (0.2 equiv. per complex **A** used) (see ESI†). When larger excess of  $\text{KC}_8$  was used (6–10 equiv.) ammonium chloride was obtained after quenching in similar yield (20–30%). Performing the reaction under  ${}^{15}\text{N}_2$  also yielded ammonium chloride ( ${}^{15}\text{NH}_4\text{Cl}$ ) in 30% yield. In contrast, no ammonium chloride formation was observed when the same reaction was performed under argon or when the reduction was carried out in hexane under dinitrogen. Moreover, the  ${}^1\text{H}$  NMR spectrum measured in  $d_8$ -toluene at  $-40$  °C of the reaction mixture obtained after reaction of **A** with 2.2 equiv. of  $\text{KC}_8$  in diethyl ether  $-40$  °C under argon showed the resonances assigned to **2** (Fig. S24b†).

Finally, the reduction of the complex **A** in benzene prevented the C–N oxidative addition from occurring leading instead to the isolation of the inverse sandwich complex  $[\{\text{U}(\kappa^5\text{–}\{({}^t\text{Bu}_2\text{ArO})_2\text{Me}_2\text{-cyclam}\})\}_2(\mu\text{-}\eta^6\text{:}\eta^6\text{-benzene})]$  (**3**) in 32% yield, formed from the

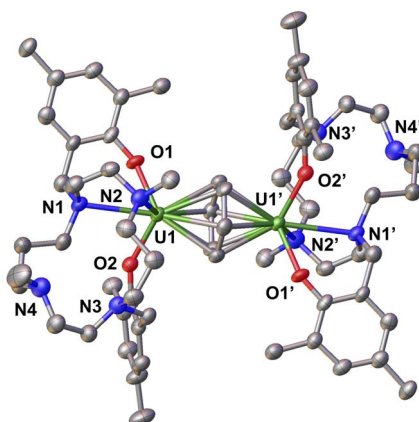


Fig. 4 Molecular structure of complex **3** with thermal ellipsoids drawn at the 50% probability level. Methyl groups of  ${}^t\text{Bu}$  group and hydrogen atoms have been omitted for clarity.

reduction of the benzene molecule by the putative U(II) intermediate. Analogous uranium inverse sandwich complexes have been reported by several groups<sup>34,36,37,59–63</sup> and are considered to be U(II) synthons because they can function as four electron reductants with diverse substrates; spectroscopic and structural studies led to the assignment of their electronic structure as consistent of U(III) centres and a dianionic bridging arene. Single crystals of **3** suitable for X-ray diffraction were isolated from a concentrated reaction mixture in toluene at  $-40$  °C (see Fig. 4). The reduction of **A** was also performed in hexane (both at  $-40$  °C and r.t.) to isolate the putative U(II). Reduction of **A** in hexane with 2.2 equiv.  $\text{KC}_8$  at r.t. over three days resulted in a dark red brown suspension. The  ${}^1\text{H}$  NMR spectrum (Fig. S23†) of the crude reaction mixture in  $d_6$ -benzene at r.t showed the presence of complex **3** as the only identifiable species suggesting that the low solubility of the putative U(II) complex in hexane prevents the reductive cleavage of the ligand. Dissolution of the residue in a more polar solvent such as  $d_8$ -THF resulted in the observation of the signals assigned to complex **2** by  ${}^1\text{H}$  NMR spectroscopy (see ESI, Fig. S16c†), signifying that the intramolecular C–N cleavage step is instantaneous in  $d_8$ -THF.

The solid-state molecular structure of **3** (see Fig. 4) reveals that each uranium metal centre is coordinated by two aryloxide oxygen atoms and two nitrogen atoms of the cyclam ring, with a benzene molecule bridging the two uranium centres. In each half of the complex, only two out of the four nitrogen atoms in the cyclam ring interact with the uranium ion in order to accommodate the benzene moiety: thereby exhibiting a conformationally flexible cyclam backbone. The U–O<sub>aryloxide</sub> bond lengths ( $2.207(3)$  Å and  $2.229(4)$  Å) are comparable to those found in complex **A** ( $2.223(4)$  Å and  $2.263(3)$  Å). The average U–C<sub>arene</sub> ( $2.61(2)$  Å) and C<sub>arene</sub>–C<sub>arene</sub> ( $1.430(14)$  Å) bond lengths are consistent with the previously reported diuranium(III) inverse sandwich complexes.<sup>34,36,37,63</sup>

### EPR and magnetism studies

To further elucidate the electronic structure of complex **A**, **2** and **3**, SQUID magnetometry (Fig. 5) and EPR (Fig. 6) studies were



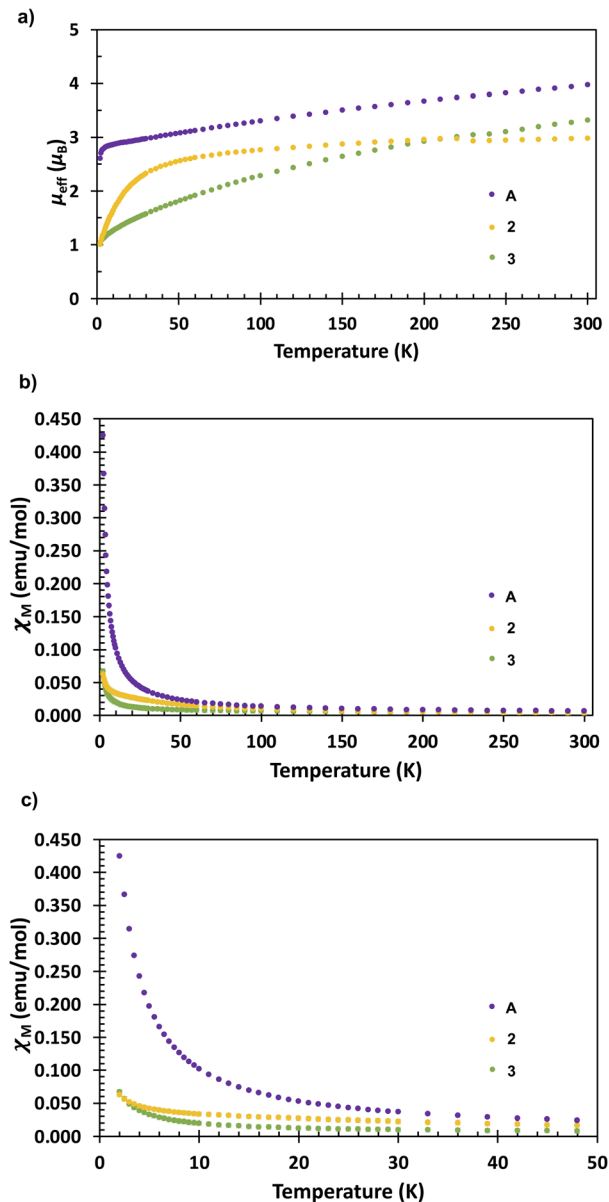


Fig. 5 Temperature dependent SQUID magnetisation data (per U ion) for complexes A, 2 and 3 plotted as functions of (a)  $\mu_{\text{eff}}$  vs. temperature, (b)  $\chi_M$  vs. temperature (where  $\chi_M$  is the molar magnetic susceptibility) and (c)  $\chi_M$  vs. temperature (shown up to 50 K only for clarity), measured at 1 T.

undertaken. Complex A has a magnetic moment of  $3.97 \mu_{\text{B}}$  ( $\chi_M = 6.58 \times 10^{-3} \text{ emu mol}^{-1}$ ;  $\chi T = 1.97 \text{ emu K mol}^{-1}$ ) at 300 K and  $2.61 \mu_{\text{B}}$  ( $\chi_M = 4.25 \times 10^{-1} \text{ emu mol}^{-1}$ ;  $\chi T = 8.50 \times 10^{-1} \text{ emu K mol}^{-1}$ ) at 2 K. The observed behaviour is similar to that reported for other U(III) compounds with an  $f^3$  electronic configuration corresponding to  $^4\text{I}_{9/2}$  ground state<sup>40,64</sup>. In such U(III) complexes the magnetic moment decreases steadily with decrease in temperature to reach a non-zero value corresponding to a doublet state for the Kramers ion. On the other hand, complex 2 has a magnetic moment of  $2.98 \mu_{\text{B}}$  ( $\chi_M = 3.70 \times 10^{-3} \text{ emu mol}^{-1}$ ;  $\chi T = 1.11 \text{ emu K mol}^{-1}$ ) at 300 K and  $1.00 \mu_{\text{B}}$  ( $\chi_M = 6.27 \times 10^{-2} \text{ emu mol}^{-1}$ ;  $\chi T = 1.25 \times 10^{-1} \text{ emu K mol}^{-1}$ ) at 2 K. The

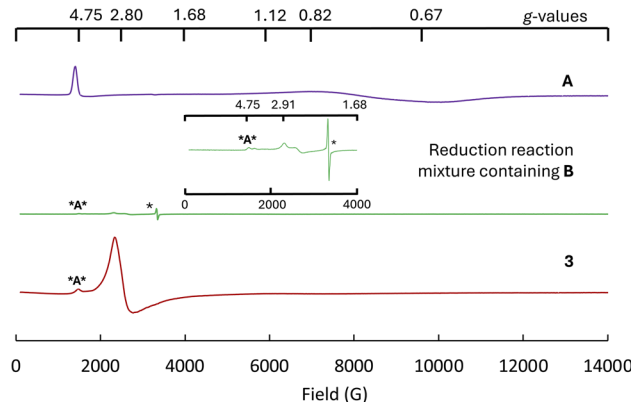


Fig. 6 Solid state X-band (9.40 GHz) EPR spectrum of: (top) A (8.0 mg), (middle) (7.2 mg) the precipitate obtained from A + 2.2  $\text{KC}_8$  reaction in hexane (which contains the intermediate species B) and (bottom) 3 (8.0 mg) at 6 K (\* corresponds to a signal arising from the itinerant electrons in the  $\text{KC}_8$ ). For clarity, the inset depicts the low-field portion (0–4000 G) of the middle spectrum, which encompasses resonance features with high g-factor values. The signal \*A\* at  $g = \sim 4.75$  in the low-field sections of the EPR spectra corresponds to denote the residual content of the complex A.

decrease in magnetic moment is more abrupt for complex 2 below 50 K, when compared to complex A. Such a decrease in magnetic moment below 50 K is well documented for various U(IV) complexes reported in the literature.<sup>64</sup> The magnetic moment for 2 does not approach zero at 2 K, which could indicate the presence of a non-singlet ground state.<sup>65</sup> Nonetheless, the magnetic data for 2 compare well with those of several U(IV) complexes reported previously.<sup>66–69</sup> In comparison, the measured magnetic moment of 3 is of  $3.32 \mu_{\text{B}}$  ( $\chi_M = 4.58 \times 10^{-3} \text{ emu mol}^{-1}$ ;  $\chi T = 1.37 \text{ emu K mol}^{-1}$ ) at 300 K and  $1.04 \mu_{\text{B}}$  ( $\chi_M = 6.70 \times 10^{-2} \text{ emu mol}^{-1}$ ;  $\chi T = 1.34 \times 10^{-1} \text{ emu K mol}^{-1}$ ) at 2 K per uranium ion, while per complex it is  $4.69 \mu_{\text{B}}$  ( $\chi_M = 9.17 \times 10^{-3} \text{ emu mol}^{-1}$ ;  $\chi T = 2.75 \text{ emu K mol}^{-1}$ ) at 300 K and  $1.46 \mu_{\text{B}}$  ( $\chi_M = 1.34 \times 10^{-1} \text{ emu mol}^{-1}$ ;  $\chi T = 2.68 \times 10^{-1} \text{ emu K mol}^{-1}$ ) at 2 K. Although the decrease in magnetic moment with the decrease in temperature in 3 is quite different from both complexes A and 2, the low value of its magnetic moment at 2 K is close to that of the U(IV) complex 2. This correlates well with DFT studies (*vide infra*) with complex 3 calculated to have a U(IV)-arene<sup>4-</sup>-U(IV) ground state but with a very close in energy U(III)-arene<sup>2-</sup>-U(III) state. Considering that an EPR signal is also observed (see next section) that can be assigned to the U(III) species is likely that both configurations contribute to the magnetic response. The observed behaviour is rather different from that reported for the analogous arene-bridged complex  $[(\mu\text{-toluene})\text{U}_2(\text{N}^{\text{t-Bu}}\text{Ar})_4]$  (Ar = 3,5-C<sub>6</sub>H<sub>3</sub>Me<sub>2</sub>) that presented a strong antiferromagnetic behaviour below 125 K and lower magnetic moment in all 5–300 K temperature range (1.57  $\mu_{\text{B}}$  at 300 K and 0.25  $\mu_{\text{B}}$  at 5 K for one uranium center).<sup>36,61</sup>

The EPR spectrum of complex A at 6 K features g-values of 4.75, 0.82 and 0.65 at 6 K (Fig. 6). EPR spectra with rhombic signals and similar low field g-factors have been reported for heteroleptic uranium(III) complexes supported by tris(3,5-dimethyl-1-pyrazolyl)borate ligands or amide ligands.<sup>70,71</sup>

While assignment of oxidation state is not trivial in inverse-sandwich complexes, EPR data measured in the solid state (Fig. 6) and in frozen solution (see ESI†) at 6 K show for complex 3 the presence of a signal in agreement with the presence of a  $f^3$  U(III) rather than EPR silent  $f^2$  U(IV) or  $f^4$  U(II) ions. The EPR spectrum of 3 at 6 K features  $g$ -values of 2.80, 2.60 and 0.8 (Fig. 6), which following spin quantification accounts for 40% of the total expected spins. Similar EPR spectra have been reported for monometallic uranium(III) complexes featuring strong donor ligands.<sup>8,72,73</sup> The observation of this EPR profile is suggestive of a U(III)-arene<sup>2-</sup>U(III) structure for complex 3 similar to the structure proposed for the inverse sandwich complex  $[(\mu\text{-toluene})\text{U}_2(\text{N}^{\text{'}}\text{Bu})\text{Ar}_4]$  complex.<sup>61</sup> The presence of such species is corroborated by the computational studies indicating the possible existence of U(III)-arene<sup>2-</sup>U(III) and U(IV)-arene<sup>4-</sup>U(IV) structures in equilibrium. Moreover, the EPR spectrum of the putative U(II) species obtained as highly insoluble solid upon reacting **A** with 2.2 KC<sub>8</sub> in hexane was also recorded to further characterize the nature of this intermediate. The EPR spectrum shows a radical-like signal due to the presence of unreacted KC<sub>8</sub> at  $g = 2.0021$  and two additional signals of very low intensity at  $g = 2.82$  and 2.52. The signals are significantly shifted with respect to the spectrum of complex **A** (a small residual signal corresponding to **A** is also observed (Fig. S40†)). The observed low intensity signals (4% integrated spins) could be tentatively assigned to the U(II) species generated upon reduction. The possibility that the signal could be arising from metallic impurity contained in KC<sub>8</sub> (ref. 74) was ruled out by measuring the solid state EPR of the same batch of KC<sub>8</sub> which revealed only an asymmetric signal at  $g = 2.0020$ , thus pointing to the itinerant electrons in the highly conducting particles of KC<sub>8</sub>. Several U(II) complexes were reported to possess a  $5f^4$  configuration<sup>1,7,8,11</sup> that did not feature any metal based EPR signal. However, recently Evans and co-workers reported EPR studies on 10 U(II) complexes having a  $5f^36d^1$  electronic configuration that showed display two-line axial signals with  $g_{\parallel} = 2.04$  and  $g_{\perp} = 2.00$ .<sup>75</sup> The reported studies suggested that the presence of EPR signals can be used to differentiate  $5f^36d^1$  and  $5f^4$  configurations in U(II) complexes.

The almost silent EPR spectrum of the product of the reduction of **A** in hexane indicate that a U(II) species is formed which is mostly in a  $5f^4$  configuration. The observed low intensity signals could suggest some contribution of the  $5f^36d^1$  configuration, because of the f-d mixing also found in the computed structure (see below). To further corroborate our hypothesis the precipitate obtained from the reduction reaction mixture was suspended in benzene and the EPR spectrum of the resulting dark red brown solution (following filtration to remove excess KC<sub>8</sub> and graphite) was measured at 6 K. The signal corresponding to the U(II) intermediate disappeared, and the signal corresponding to complex 3 was observed in the EPR spectrum recorded (Fig. S27†). These results provide further evidence of the involvement of a U(II) species in both reduction of benzene observed in 3 and the N-C cleavage observed in the case of 2.

## Computational studies

DFT studies were carried out (B3PW91 functional) to give some insights on the formation of complex 2 and the electronic structure of complex 3. First of all the formation of the U(II) intermediate **B** was investigated computationally. Although disproportionation of the starting complex **A** is prohibitively high (68.0 kcal mol<sup>-1</sup> in enthalpy and 68.9 kcal mol<sup>-1</sup> in Gibbs Free Energy), the reduction of complex **A** to form the transient complex **B** is endothermic by 23.4 kcal mol<sup>-1</sup> in enthalpy (19.5 kcal mol<sup>-1</sup> in Gibbs Free Energy). In THF solution, this reaction is becoming endothermic by 15.2 kcal mol<sup>-1</sup> in enthalpy (11.1 kcal mol<sup>-1</sup> in Gibbs Free energy). This makes this intermediate plausible and it is in line with the fact that this transient species was not experimentally stabilised. The electronic structure of **B** clearly indicates a U(II) system in a  $S = 2$  ground state. The associated electronic configuration is a mixture of the  $5f^4$  and  $5f^3d^1$  configurations since three pure 5f orbitals are occupied and the fourth one is a mixture (60–40) between the  $5f_0$  and  $6d_0$  atomic orbitals. This electronic structure fits the EPR data and the hypothesis given experimentally. The formation of complex 2 from complex **B** was thus investigated (Fig. 7). In complex **B**, the coordination of both nitrogen and oxygen induces a slight elongation of the C–N bond (1.50 Å) with respect to simple amines (1.47 Å). Complex **B** can easily reach a C–N bond breaking transition state (TS2) with an accessible barrier of 16.4 kcal mol<sup>-1</sup> in enthalpy (16.9 kcal mol<sup>-1</sup> in Gibbs Free Energy). At the transition state, the C–N bond is already broken (1.88 Å) while the U–N distance is decreased to 2.55 Å. Following the intrinsic reaction

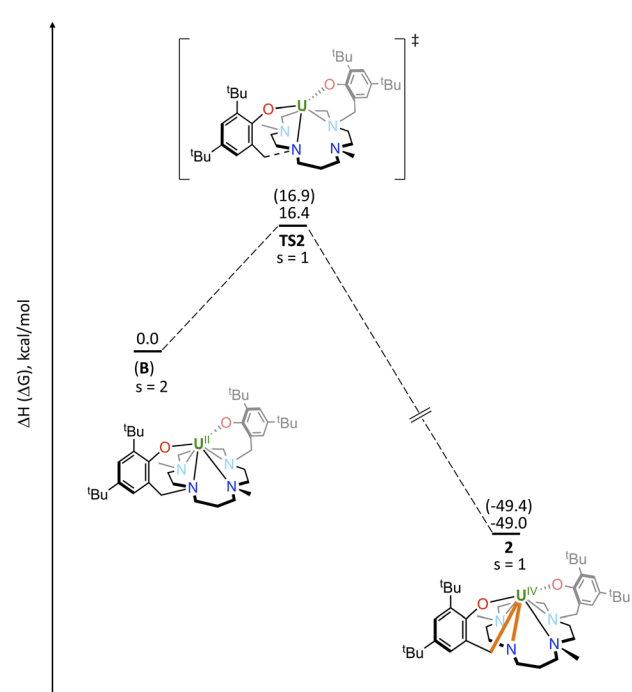


Fig. 7 Computed enthalpy profile (Gibbs free energy between bracket) at room temperature for the formation of complex 2 from intermediate **B**. The energies are given in kcal mol<sup>-1</sup>.  $S$  stands for the total spin state of each intermediate.



coordinate, it yields the very stable complex **2** ( $-49.0\text{ kcal mol}^{-1}$  in enthalpy,  $-49.4\text{ kcal mol}^{-1}$  in Gibbs Free Energy).

The electronic structure of complex **3** was finally investigated computationally using the same methodology. Two spin states were considered, namely a  $S = 3$  (two U( $\text{m}$ ) centres) and  $S = 2$  (two U( $\text{iv}$ ) centres) spin states. The  $S = 2$  (quintet) is slightly more stable than the  $S = 3$  (septet) by  $4.8\text{ kcal mol}^{-1}$  in enthalpy ( $2.5\text{ kcal mol}^{-1}$  in Gibbs Free Energy). This TS is located on the triplet Potential Energy Surface (PES) and corresponds to a U( $\text{iv}$ ). This small energy difference indicates that these two structures could be in equilibrium and that clearly both can be populated at room temperature, in agreement with the observed experimental magnetism. The comparison between the optimized geometry in both spin states and the experimental one clearly shows that the quintet geometry is the one that is in best agreement with the X-ray (see Table S4 $\dagger$ ). In both cases, the unpaired spin density plots (Fig. S47k and S48k $\dagger$ ) are located at the two uranium centres only, indicating either two U( $\text{iv}$ ) for the quintet or two U( $\text{m}$ ) for the septet. The main difference between the two spin states is the presence of two doubly occupied  $\delta$ -bonds (HOMO and HOMO – 1) for the quintet while only one is occupied (HOMO – 1) for the septet (Fig. S47 and S48 $\dagger$ ). The situation is different for  $[(\mu\text{-toluene})\text{U}_2(\text{N}[\text{Ad}]\text{Ar})_4]$  ( $\text{Ar} = 3,5\text{-C}_6\text{H}_3\text{Me}_2$ ), since the quintet is found to be the ground state while the septet is  $15.3\text{ kcal mol}^{-1}$  higher in enthalpy ( $16.9\text{ kcal mol}^{-1}$  in Gibbs Free Energy). Therefore, there is no equilibrium between the two spin states, explaining the difference in magnetism observed with complex **3**.

## Conclusion

In conclusion reduction of the heteroleptic aminephenolate complex **A** in apolar solvents produces a highly reactive transient neutral "U( $\text{n}$ )" species (**B**). In contrast, upon replacement of the iodide ligand in **A** with a siloxide to yield complex **1**, the reduction of the uranium centre is not observed even in presence of excess reducing agent with only minor decomposition products formed.

In polar solvents **B** undergoes a unique example of C–N oxidative addition to a U( $\text{n}$ ) center to yield complex **2**. The transient complex **B** was also found to reduce benzene to yield the inverse sandwich complex **3**. Computational, EPR and magnetic studies indicate the presence for **3** of an equilibrium between two possible electronic structures very close in energy (U( $\text{iv}$ )-arene $^{4-}$ –U( $\text{iv}$ ) and U( $\text{m}$ )-arene $^{2-}$ –U( $\text{m}$ )). These results indicate that polydentate amine-phenolate ligands can be used to access highly reactive U( $\text{n}$ ) intermediates and that U( $\text{n}$ ) species are involved in the formation of inverse sandwich complexes. Moreover the "U( $\text{n}$ )" intermediate was found to react with  $\text{N}_2$  yielding ammonia (even if in low yield) upon acidification. Future studies will be directed to tune the stability and the reactivity of the U( $\text{n}$ ) intermediate by ligand design.

## Data availability

Synthetic details, analytical data including depictions of all spectra and coordinate data of all computationally optimised

species, are documented in the ESI. $\dagger$  Crystallographic data is made available *via* the CCDC. The data that support the findings of this study are openly available in the zenodo repository at <https://doi.org/10.5281/zenodo.15801184>. $\dagger$

## Author contributions

R. A. K. S designed and carried out all the experiments and analysed the data; L. M. carried out the ligand synthesis and some of the experiments and analysed the data. M. M. designed and supervised the project and analysed the data; T. R. and L. M. carried out the computational study; R. S. measured and analyzed the X-ray data, I. Z. measured and analysed the magnetic data; A. S. measured and analysed the EPR data; R. A. K. S and M. M. wrote the manuscript with contributions of all authors, and all authors have given approval for the final version of the manuscript.

## Conflicts of interest

There are no conflicts to declare.

## Acknowledgements

We acknowledge support from the Swiss National Science Foundation grant number 212723 and 217133 and the Ecole Polytechnique Fédérale de Lausanne (EPFL). LM is a senior member of the Institut Universitaire de France. CalMip is acknowledged for a generous grant of computing time. Leonor Maria acknowledges support from Fundação para a Ciencia e a Tecnologia (FCT) through projects UIDB/00100/2020 (CQE) and LA/P/0056/2020 (IMS). We thank Dr Maxime Tricoire for assistance with EPR data collection and analysis.

## Notes and references

- 1 H. S. La Pierre, A. Scheurer, F. W. Heinemann, W. Hieringer and K. Meyer, Synthesis and Characterization of a Uranium( $\text{n}$ ) Monoarene Complex Supported by delta Backbonding, *Angew. Chem., Int. Ed.*, 2014, **53**, 7158–7162.
- 2 M. R. MacDonald, M. E. Fieser, J. E. Bates, J. W. Ziller, F. Furche and W. J. Evans, Identification of the +2 Oxidation State for Uranium in a Crystalline Molecular Complex, K(2.2.2-Cryptand) (C<sub>5</sub>H<sub>4</sub>SiMe<sub>3</sub>)<sub>3</sub>U, *J. Am. Chem. Soc.*, 2013, **135**, 13310–13313.
- 3 F. S. Guo, N. Tsoureas, G. Z. Huang, M. L. Tong, A. Mansikkamaki and R. A. Layfield, Isolation of a Perfectly Linear Uranium( $\text{n}$ ) Metallocene, *Angew. Chem., Int. Ed.*, 2020, **59**, 2299–2303.
- 4 A. J. Ryan, M. A. Angadol, J. W. Ziller and W. J. Evans, Isolation of U( $\text{n}$ ) compounds using strong donor ligands, C<sub>5</sub>Me<sub>4</sub>H and N(SiMe<sub>3</sub>)<sub>2</sub>, including a three-coordinate U( $\text{n}$ ) complex, *Chem. Commun.*, 2019, **55**, 2325–2327.
- 5 D. N. Huh, J. W. Ziller and W. J. Evans, Chelate-Free Synthesis of the U( $\text{n}$ ) Complex, (C<sub>5</sub>H<sub>3</sub>(SiMe<sub>3</sub>)<sub>2</sub>)<sub>3</sub>U (1–), Using Li and Cs Reductants and Comparative Studies of

La(II) and Ce(II) Analogs, *Inorg. Chem.*, 2018, **57**, 11809–11814.

6 D. N. Huh, C. J. Windorff, J. W. Ziller and W. J. Evans, Synthesis of uranium-in-cryptand complexes, *Chem. Commun.*, 2018, **54**, 10272–10275.

7 B. S. Billow, B. N. Livesay, C. C. Mokhtarzadeh, J. McCracken, M. P. Shores, J. M. Boncella and A. L. Odom, Synthesis and Characterization of a Neutral U(n) Arene Sandwich Complex, *J. Am. Chem. Soc.*, 2018, **140**, 17369–17373.

8 M. Keener, R. A. K. Shivaraam, T. Rajeshkumar, M. Tricoire, R. Scopelliti, I. Zivkovic, A. S. Chauvin, L. Maron and M. Mazzanti, Multielectron Redox Chemistry of Uranium by Accessing the plus II Oxidation State and Enabling Reduction to a U(I) Synthon, *J. Am. Chem. Soc.*, 2023, **145**, 16271–16283.

9 C. Deng, J. F. Liang, R. Sun, Y. Wang, P. X. Fu, B. W. Wang, S. Gao and W. L. Huang, Accessing five oxidation states of uranium in a retained ligand framework, *Nat. Commun.*, 2023, **14**, 4657.

10 N. Tsoureas and I. Vagiakos, Recent Advances in Low Valent Thorium and Uranium Chemistry, *Inorganics*, 2024, **12**, 275.

11 M. D. Straub, E. T. Ouellette, M. A. Boreen, R. D. Britt, K. Chakarawet, I. Douair, C. A. Gould, L. Maron, I. Del Rosal, D. Villarreal, S. G. Minasian and J. Arnold, A Uranium(II) Arene Complex That Acts as a Uranium(I) Synthon, *J. Am. Chem. Soc.*, 2021, **143**, 19748–19760.

12 D. K. Modder, C. T. Palumbo, I. Douair, R. Scopelliti, L. Maron and M. Mazzanti, Single metal four-electron reduction by U(II) and masked “U(II)” compounds, *Chem. Sci.*, 2021, **12**, 6153–6158.

13 H. S. La Pierre, H. Kameo, D. P. Halter, F. W. Heinemann and K. Meyer, Coordination and Redox Isomerization in the Reduction of a Uranium(III) Monoarene Complex, *Angew. Chem., Int. Ed.*, 2014, **53**, 7154–7157.

14 J. C. Wedal, J. W. Ziller, F. Furche and W. J. Evans, Synthesis and Reduction of Heteroleptic Bis(cyclopentadienyl) Uranium(III) Complexes, *Inorg. Chem.*, 2022, **61**, 7365–7376.

15 J. C. Wedal, S. Bekoe, J. W. Ziller, F. Furche and W. J. Evans, C-H Bond Activation via U(II) in the Reduction of Heteroleptic Bis(trimethylsilyl)amide U(III) Complexes, *Organometallics*, 2020, **39**, 3425–3432.

16 M. A. Boreen, C. S. Z. Ye, A. Kerridge, K. N. McCabe, B. A. Skeel, L. Maron and J. Arnold, Does Reduction-Induced Isomerization of a Uranium(III) Aryl Complex Proceed via C-H Oxidative Addition and Reductive Elimination across the Uranium(II/IV) Redox Couple?, *Inorg. Chem.*, 2022, **61**, 8955–8965.

17 W. Fang, Y. F. Li, T. Z. Zhang, T. Rajeshkumar, I. del Rosal, Y. Zhao, T. W. Wang, S. O. Wang, L. Maron and C. Q. Zhu, Oxidative Addition of E-H (E = C, N) Bonds to Transient Uranium(II) Centers, *Angew. Chem., Int. Ed.*, 2024, **63**, e202419987.

18 C. Deng, Y. L. Li, Y. Wang and W. L. Huang, Two-Electron Oxidative Atom and Group Transfer Reactions at a Well-Defined Uranium(II) Center, *Angew. Chem. Int. Ed. Engl.*, 2025, **64**, e202419987.

19 J. F. Hartwig, *Organotransition Metal Chemistry*, University Science Books, New York, 2010.

20 B. M. Gardner, C. E. Kefalidis, E. Lu, D. Patel, E. J. L. McInnes, F. Tuna, A. J. Wooley, L. Maron and S. T. Liddle, Evidence for single metal two electron oxidative addition and reductive elimination at uranium, *Nat. Commun.*, 2017, **8**, 1898.

21 E. Lu and S. T. Liddle, Uranium-mediated oxidative addition and reductive elimination, *Dalton Trans.*, 2015, **44**, 12924–12941.

22 C. L. Webster, J. W. Ziller and W. J. Evans, Reactivity of U3+ Metallocene Allyl Complexes Leads to a Nanometer-Sized Uranium Carbonate, (C5Me5)(2)U (6)(mu-kappa(1):kappa(2)-CO3)(6), *Organometallics*, 2013, **32**, 4820–4827.

23 D. R. Hartline, S. T. Löftier, D. Fehn, J. M. Kasper, F. W. Heinemann, P. Yang, E. R. Batista and K. Meyer, Uranium-Mediated Peroxide Activation and a Precursor toward an Elusive Uranium cis-Dioxo Fleeting Intermediate, *J. Am. Chem. Soc.*, 2023, **145**, 8927–8938.

24 I. Korobkov, S. Gambarotta and G. P. A. Yap, A highly reactive uranium complex supported by the calix 4 tetrapyrrole tetraanion affording dinitrogen cleavage, solvent deoxygenation, and polysilanol depolymerization, *Angew. Chem., Int. Ed.*, 2002, **41**, 3433–3436.

25 I. Korobkov, S. Gambarotta and G. P. A. Yap, Highly reactive uranium(III) polypyrrrolide complexes: intramolecular C-H bond activation, ligand isomerization, and solvent deoxygenation and fragmentation, *Organometallics*, 2001, **20**, 2552–2559.

26 B. P. Warner, B. L. Scott and C. J. Burns, A simple preparative route to bis(imido)-uranium(VI) complexes by the direct reductions of diazenes and azides, *Angew. Chem., Int. Ed.*, 1998, **37**, 959–960.

27 M. Falcone, L. Chatelain, R. Scopelliti, I. Zivkovic and M. Mazzanti, Nitrogen reduction and functionalization by a multimetallic uranium nitride complex, *Nature*, 2017, **547**, 332–335.

28 J. J. Kiernicki, P. E. Fanwick and S. C. Bart, Utility of a redox-active pyridine(diimine) chelate in facilitating two electron oxidative addition chemistry at uranium, *Chem. Commun.*, 2014, **50**, 8189–8192.

29 E. M. Matson, S. R. Opperwall, P. E. Fanwick and S. C. Bart, “Oxidative Addition” of Halogens to Uranium(IV) Bis(amidophenolate) Complexes, *Inorg. Chem.*, 2013, **52**, 7295–7304.

30 D. P. Halter, F. W. Heinemann, L. Maron and K. Meyer, The role of uranium-arene bonding in H<sub>2</sub>O reduction catalysis, *Nat. Chem.*, 2018, **10**, 259–267.

31 N. H. Anderson, S. O. Odoh, Y. Y. Yao, U. J. Williams, B. A. Schaefer, J. J. Kiernicki, A. J. Lewis, M. D. Goshert, P. E. Fanwick, E. J. Schelter, J. R. Walensky, L. Gagliardi and S. C. Bart, Harnessing redox activity for the formation of uranium tris(imido) compounds, *Nat. Chem.*, 2014, **6**, 919–926.



32 W. J. Evans and B. L. Davis, Chemistry of tris(pentamethylcyclopentadienyl) f-element complexes,  $(C_5Me_5)_3M$ , *Chem. Rev.*, 2002, **102**, 2119–2136.

33 W. J. Evans, S. A. Kozimor and J. W. Ziller,  $(C_5Me_5)_2U$  (mu-Ph)(2)BPh<sub>2</sub> as a four electron reductant, *Chem. Commun.*, 2005, 4681–4683.

34 S. T. Liddle, Inverted sandwich arene complexes of uranium, *Coord. Chem. Rev.*, 2015, **293**, 211–227.

35 P. L. Diaconescu and C. C. Cummins, Diuranium inverted sandwiches involving naphthalene and cyclooctatetraene, *J. Am. Chem. Soc.*, 2002, **124**, 7660–7661.

36 P. L. Diaconescu, P. L. Arnold, T. A. Baker, D. J. Mindiola and C. C. Cummins, Arene-bridged diuranium complexes: Inverted sandwiches supported by delta backbonding, *J. Am. Chem. Soc.*, 2000, **122**, 6108–6109.

37 W. J. Evans, S. A. Kozimor, J. W. Ziller and N. Kaltsoyannis, Structure, reactivity, and density functional theory analysis of the six-electron reductant,  $(C_5Me_5)_2U$  (2)(mu-eta(6):eta(6)-C<sub>6</sub>H<sub>6</sub>), synthesized via a new mode of  $(C_5Me_5)_3M$  reactivity, *J. Am. Chem. Soc.*, 2004, **126**, 14533–14547.

38 C. J. Windorff, M. R. MacDonald, K. R. Meihaus, J. W. Ziller, J. R. Long and W. J. Evans, Expanding the Chemistry of Molecular U<sup>2+</sup> Complexes: Synthesis, Characterization, and Reactivity of the  $\{C_5H_3(SiMe_3)_2\} (3)U(-)$  Anion, *Chem.-Eur. J.*, 2016, **22**, 772–782.

39 D. K. Modder, R. Scopelliti and M. Mazzanti, Accessing a Highly Reducing Uranium(III) Complex through Cyclometalation, *Inorg. Chem.*, 2024, **63**, 9527–9538.

40 I. Castro-Rodriguez and K. Meyer, Small molecule activation at uranium coordination complexes: control of reactivity via molecular architecture, *Chem. Commun.*, 2006, 1353–1368.

41 L. Maria, I. C. Santos, V. R. Sousa and J. Marcalo, Uranium(III) Redox Chemistry Assisted by a Hemilabile Bis(phenolate) Cyclam Ligand: Uranium-Nitrogen Multiple Bond Formation Comprising a trans-{RN=U(vi)=NR}(2+) Complex, *Inorg. Chem.*, 2015, **54**, 9115–9126.

42 A. N. Desnoyer and J. A. Love, Recent advances in well-defined, late transition metal complexes that make and/or break C–N, C–O and C–S bonds, *Chem. Soc. Rev.*, 2017, **46**, 197–238.

43 J. García-Cárceles, K. A. Bahou and J. F. Bower, Recent Methodologies That Exploit Oxidative Addition of C–N Bonds to Transition Metals, *ACS Catal.*, 2020, **10**, 12738–12759.

44 K. B. Ouyang, W. Hao, W. X. Zhang and Z. F. Xi, Transition-Metal-Catalyzed Cleavage of C–N Single Bonds, *Chem. Rev.*, 2015, **115**, 12045–12090.

45 O. V. Ozerov, C. Y. Guo, V. A. Papkov and B. M. Foxman, Facile oxidative addition of N–C and N–H bonds to monovalent rhodium and iridium, *J. Am. Chem. Soc.*, 2004, **126**, 4792–4793.

46 T. M. Cameron, K. A. Abboud and J. M. Boncella, Unusual molybdenum mediated C–N bond activation, *Chem. Commun.*, 2001, 1224–1225.

47 J. B. Bonanno, T. P. Henry, D. R. Neithamer, P. T. Wolezanski and E. B. Lobkovsky, Arylamine C–N bond oxidative addition to (silox)(3)Ta (silox = (t)Bu(3)SiO), *J. Am. Chem. Soc.*, 1996, **118**, 5132–5133.

48 D. Patel, F. Moro, J. McMaster, W. Lewis, A. J. Blake and S. T. Liddle, A Formal High Oxidation State Inverse-Sandwich Diuranium Complex: A New Route to f-Block-Metal Bonds, *Angew. Chem., Int. Ed.*, 2011, **50**, 10388–10392.

49 S. Fortier, J. L. Brown, N. Kaltsoyannis, G. Wu and T. W. Hayton, Synthesis, Molecular and Electronic Structure of U–V(O) N(SiMe<sub>3</sub>)<sub>2</sub>(3), *Inorg. Chem.*, 2012, **51**, 1625–1633.

50 C. J. Windorff, J. M. Sperling, T. E. Albrecht-Schönzart, Z. L. Bai, W. J. Evans, A. N. Gaiser, A. J. Gaunt, C. A. P. Goodwin, D. E. Hobart, Z. K. Huffman, D. N. Huh, B. E. Klamm, T. N. Poe and E. Warzecha, A Single Small-Scale Plutonium Redox Reaction System Yields Three Crystallographically-Characterizable Organoplutonium Complexes, *Inorg. Chem.*, 2020, **59**, 13301–13314.

51 E. J. Schelter, R. L. Wu, B. L. Scott, J. D. Thompson, T. Cantat, K. D. John, E. R. Batista, D. E. Morris and J. L. Kiplinger, Actinide Redox-Active Ligand Complexes: Reversible Intramolecular Electron-Transfer in U(dpp-BIAN)(2)/U(dpp-BIAN)(2)(THF), *Inorg. Chem.*, 2010, **49**, 924–933.

52 S. Fortier, B. C. Melot, G. Wu and T. W. Hayton, Homoleptic Uranium(IV) Alkyl Complexes: Synthesis and Characterization, *J. Am. Chem. Soc.*, 2009, **131**, 15512–15521.

53 L. A. Seaman, J. R. Walensky, G. Wu and T. W. Hayton, In Pursuit of Homoleptic Actinide Alkyl Complexes, *Inorg. Chem.*, 2013, **52**, 3556–3564.

54 P. L. Diaconescu, A. L. Odom, T. Agapie and C. C. Cummins, Uranium-group 14 element single bonds: isolation and characterization of a uranium(IV) silyl species, *Organometallics*, 2001, **20**, 4993–4995.

55 S. Duhovic, J. V. Oria, S. O. Odoh, G. Schreckenbach, E. R. Batista and P. L. Diaconescu, Investigation of the Electronic Structure of Mono(1,1'-Diamidoferrocene) Uranium(IV) Complexes, *Organometallics*, 2013, **32**, 6012–6021.

56 E. J. Schelter, J. M. Veauthier, C. R. Graves, K. D. John, B. L. Scott, J. D. Thompson, J. A. Pool-Davis-Tourneau, D. E. Morris and J. L. Kiplinger, 1,4-Dicyanobenzene as a scaffold for the preparation of bimetallic actinide complexes exhibiting metal–metal communication, *Chem.-Eur. J.*, 2008, **14**, 7782–7790.

57 K. C. Jantunen, C. J. Burns, I. Castro-Rodriguez, R. E. Da Re, J. T. Golden, D. E. Morris, B. L. Scott, F. L. Taw and J. L. Kiplinger, Thorium(IV) and uranium(IV) ketimide complexes prepared by nitrile insertion into actinide-alkyl and -aryl bonds, *Organometallics*, 2004, **23**, 4682–4692.

58 B. S. Newell, T. C. Schwaab and M. P. Shores, Synthesis and Characterization of a Novel Tetranuclear 5f Compound: A New Synthon for Exploring U(IV) Chemistry, *Inorg. Chem.*, 2011, **50**, 12108–12115.

59 A. J. Woole, D. P. Mills, F. Tuna, E. J. L. McInnes, G. T. W. Law, A. J. Fuller, F. Kremer, M. Ridgway, W. Lewis, L. Gagliardi, B. Vlaisavljevich and S. T. Liddle, Uranium(III)–carbon multiple bonding supported by arene



delta-bonding in mixed-valence hexauranium nanometre-scale rings, *Nat. Commun.*, 2018, **9**, 2097.

60 D. P. Mills, F. Moro, J. McMaster, J. van Slageren, W. Lewis, A. J. Blake and S. T. Liddle, A delocalized arene-bridged diuranium single-molecule magnet, *Nat. Chem.*, 2011, **3**, 454–460.

61 B. Vlaisayljevich, P. L. Diaconescu, W. L. Lukens Jr, L. Gagliardi and C. C. Cummins, Investigations of the Electronic Structure of Arene-Bridged Diuranium Complexes, *Organometallics*, 2013, **32**, 1341–1352.

62 M. J. Monreal, S. I. Khan, J. L. Kiplinger and P. L. Diaconescu, Molecular quadrangle formation from a diuranium mu-eta(6),eta(6)-toluene complex, *Chem. Commun.*, 2011, **47**, 9119–9121.

63 W. J. Evans, C. A. Traina and J. W. Ziller, Synthesis of Heteroleptic Uranium (mu-eta(6):eta(6)-C<sub>6</sub>H<sub>6</sub>)(2-) Sandwich Complexes via Facile Displacement of (eta(5)-C<sub>5</sub>Me<sub>5</sub>)(1-) by Ligands of Lower Hapticity and Their Conversion to Heteroleptic Bis(imido) Compounds, *J. Am. Chem. Soc.*, 2009, **131**, 17473–17481.

64 D. R. Kindra and W. J. Evans, Magnetic Susceptibility of Uranium Complexes, *Chem. Rev.*, 2014, **114**, 8865–8882.

65 J. A. Seed, L. Birnoschi, E. L. Lu, F. Tuna, A. J. Woole, N. F. Chilton and S. T. Liddle, Anomalous magnetism of uranium(IV)-oxo and -imido complexes reveals unusual doubly degenerate electronic ground states, *Chem.*, 2021, **7**, 1666–1680.

66 I. Castro-Rodriguez, H. Nakai and K. Meyer, Multiple-bond metathesis mediated by sterically pressured uranium complexes, *Angew. Chem. Int. Ed. Engl.*, 2006, **45**, 2389–2392.

67 S. C. Bart, F. W. Heinemann, C. Anthon, C. Hauser and K. Meyer, A New Tripodal Ligand System with Steric and Electronic Modularity for Uranium Coordination Chemistry, *Inorg. Chem.*, 2009, **48**, 9419–9426.

68 O. P. Lam, P. L. Feng, F. W. Heinemann, J. M. O'Connor and K. Meyer, Charge-separation in uranium diazomethane complexes leading to C–H activation and chemical transformation, *J. Am. Chem. Soc.*, 2008, **130**, 2806–2816.

69 E. M. Matson, M. D. Goshert, J. J. Kiernicki, B. S. Newell, P. E. Fanwick, M. P. Shores, J. R. Walensky and S. C. Bart, Synthesis of Terminal Uranium(IV) Disulfido and Diselenido Compounds by Activation of Elemental Sulfur and Selenium, *Chem.–Eur. J.*, 2013, **19**, 16176–16180.

70 J. A. Seed, M. Gregson, F. Tuna, N. F. Chilton, A. J. Woole, E. J. L. McInnes and S. T. Liddle, Rare-Earth- and Uranium-Mesoionic Carbene: A New Class of f-Block Carbene Complex Derived from an N-Heterocyclic Olefin, *Angew. Chem., Int. Ed.*, 2017, **56**, 11534–11538.

71 N. J. Wolford, X. J. Yu, S. C. Bart, J. Autschbach and M. L. Neidig, Ligand effects on electronic structure and bonding in U(III) coordination complexes: a combined MCD, EPR and computational study, *Dalton Trans.*, 2020, **49**, 14401–14410.

72 W. W. Lukens, M. Speldrich, P. Yang, T. J. Duignan, J. Autschbach and P. Kogerler, The roles of 4f-and 5f-orbitals in bonding: a magnetochemical, crystal field, density functional theory, and multi-reference wavefunction study, *Dalton Trans.*, 2016, **45**, 11508–11521.

73 D. Pividori, M. E. Miehlich, B. Kestel, F. W. Heinemann, A. Scheurer, M. Patzschke and K. Meyer, Uranium Going the Soft Way: Low-Valent Uranium(III) Coordinated to an Arene-Anchored Tris-Thiophenolate Ligand, *Inorg. Chem.*, 2021, **60**, 16455–16465.

74 A. Ambrosi, C. K. Chua, B. Khezri, Z. Sofer, R. D. Webster and M. Pumera, Chemically reduced graphene contains inherent metallic impurities present in parent natural and synthetic graphite, *Proc. Natl. Acad. Sci. USA*, 2012, **109**, 12899–12904.

75 J. C. Wedal, W. N. G. Moore, W. W. Lukens and W. J. Evans, Perplexing EPR Signals from 5f<sup>3</sup>6d<sup>1</sup> U(II) Complexes, *Inorg. Chem.*, 2024, **63**, 2945–2953.

